1983

Observed interrelations between 10m winds, ocean whitecaps and marine aerosols

Monahan, Edward C.; Fairall, Christopher W.; Davidson, Kenneth L.; Boyle, Patricia Jones

Royal Meteorological Society

Monahan, Edward C., et al. "Observed interrelations between 10m winds, ocean whitecaps and marine aerosols." Quarterly Journal of the Royal Meteorological Society 109.460 (1983): 379-392.
http://hdl.handle.net/10945/61580

Quart. J. R. Met. Soc. (1983), **109**, pp. 379–392

551.556.8:551.574.11:551.465.74

Observed inter-relations between 10 m winds, ocean whitecaps and marine aerosols

By EDWARD C. MONAHAN,[1,3] CHRISTOPHER W. FAIRALL,[2,4] KENNETH L. DAVIDSON[1] and PATRICIA JONES BOYLE[1]

(Received 16 February 1982; revised 8 December 1982)

SUMMARY

Low elevation aerosol spectra, ocean whitecap cover and 10 m wind speeds measured during the 1978 JASIN experiment have been inter-related and compared with previously published observations. The positive dependence of aerosol concentration upon whitecap cover was found to increase with droplet radius reflecting the expected higher correlation of the concentration of larger droplets, which have shorter effective residence time in the marine atmospheric boundary layer, with the immediate whitecap cover, which reflects the instantaneous rate of aerosol generation at the sea surface. The power-law wind dependence, U^{λ}, of the low elevation concentration of droplets larger than 8 μm radius was determined to be similar to the wind dependence of whitecap cover, with λ values of 3·23 and 3·31 resulting from the respective application of the robust bi-weight fitting technique. This observation is consonant with an aerosol generation model in which the instantaneous rate of production is simply proportional to the immediate whitecap cover.

The large droplet end of the JASIN low elevation aerosol spectrum is seen to undergo a marked enhancement when the wind speed exceeds 10 m s^{-1}. This is a consequence of the onset at that speed of supplementary droplet production via the mechanical disruption of wave crests. The observed growth, with increasing wind speed, in the disparity in amplitude of near-sea-surface and near-cloud-base aerosol spectra is in part a consequence of the fact that the larger droplets, produced in relative abundance at the higher wind speeds, fall out before they can be mixed effectively through the boundary layer.

1. INTRODUCTION

It has been acknowledged for at least a century that the larger marine aerosols are primarily sea-salt particles and salt-water droplets which have been 'taken up from the waves by the wind' (Sigerson 1870). Two specific mechanisms, both associated with the bursting of whitecap bubbles, have long been deemed responsible for the introduction of most of the salt droplets into the marine atmospheric boundary layer. The contribution of film droplets, produced during the rupture of the bubble cap, to the marine aerosol ensemble has been considered by Moore and Mason (1954), Blanchard (1963), Cipriano and Blanchard (1981) and numerous others. The injection of jet drops into the lowest 0·18 m of the marine atmosphere by the vertical jet formed upon the collapse of a whitecap bubble has been studied in detail by, among others, Kientzler *et al.* (1954), Blanchard and Woodcock (1957), Hayami and Toba (1958). Both these whitecap-related mechanisms of aerosol production have recently been reviewed by Wu (1979a), Coantic (1980) and Blanchard and Woodcock (1980).

In the light of the clearly perceived association of ocean whitecap cover with marine aerosol production, the existence of only a very few collections of ship-board observations that include simultaneous records of marine aerosol concentration and ocean whitecap cover must be considered a serious deficiency. During the Joint Air–Sea Interaction experiment (JASIN) recently carried out in the vicinity of Rockall, aerosols were sampled, whitecaps were photographically recorded, and a variety of meteorological measurements appropriate for air–sea exchange estimates were made aboard the *R.R.S. Challenger*. The only previously reported research cruise programme that included both aerosol and whitecap observations was that carried out aboard the *R.V. Hakuho Maru* in the East China Sea and in the coastal waters of Japan (Chaen 1973; Toba and Chaen 1973).

The immediate purpose of this paper is to describe the inter-relations observed between the 10 m wind speed, the ocean whitecap cover and the concentration of sea-salt aerosols, as recorded aboard the *Challenger*, and further to compare and combine these

[1] Department of Meteorology, Naval Postgraduate School, Monterey, CA 93940
[2] BDM Corporation, Monterey, CA 93940
[3] Permanent address: Department of Oceanography, University College, Galway, Ireland
[4] Present address: Department of Meteorology, Pennsylvania State University.

data with the *Hakuho Maru* observations. Representative aerosol spectra associated with various windspeeds and sea states have been constructed from the *Challenger* data and will be compared with other relevant marine aerosol spectra, e.g. those reported in Woodcock (1953), Metnieks (1958) and Patterson *et al.* (1980).

2. Aerosol measurements

Two Particle Measuring Systems® aerosol spectrometer probes with complementary ranges of detection were used to measure sea-salt droplets during the JASIN experiment. These instruments were mounted 14 m above the water-line on the foremast of the *Challenger*. The active scattering laser probe, model ASASP-300, detected droplets with radii between 0·1 and 3 μm while the classical scattering lasar probe, model CSASP-100, sensed droplets in the 0·5 to 15 μm radius range. The ASASP-300 probe sucked air in via its intake horn at a speed of 7·2 m s^{-1}, sampling in this manner $1{\cdot}3 \times 10^{-7}$ m^3 s^{-1}. The CSASP-100 probe maintained an air sampling rate of $1{\cdot}52 \times 10^{-5}$ m^3 s^{-1} by drawing in air at a speed of 20 m s^{-1}. A microprocessor data acquisition system, P.M.S. model DAS-32, and a Hewlett–Packard computer, model 9825S, were used to collect, process and store the spectrometer data as well as data from a suite of meteorological instruments.

As a convenience in the presentation of the size spectra, and so as to be more directly applicable to the calculation of optical extinction (Schacher *et al.* 1981), these data will henceforth usually be expressed in terms of dV/dr, the fraction of the marine air volume occupied by salt-water droplets whose radii fall within a specified radius increment.

These probe measurements are subject to several unavoidable limitations. One, a concomitant of the phenomenon of Mie scattering, is that the amplitude of the near-forward-scattered light pulses detected by the aerosol probes is not a monotonic function of droplet radius (Pinnick and Auvermann 1979). Thus there are several radii ranges within which the P.M.S. system's identification of pulse amplitude with droplet radius remains ambiguous. Another limitation, present even when the sampling has extended over protracted 3600 s periods, is that the number of larger droplets detected by the CSASP-100 aerosol probe is quite small, and hence this count manifests the large random fluctuations associated with statistics of small samples. In the light of these limitations a smoothing procedure has been applied to the $\log(dV/dr)$ *v.* $\log(r)$ spectral representations of the aerosol measurements from each sampling period. This involves the uniform rejection of aerosol measurements in certain radii categories subject to the aforementioned ambiguity, the generation by extrapolation of aerosol values for two radii beyond the actual range of measurement, i.e. 0·03 and 32 μm, and then the fitting of a seventh-order polynomial to the resulting points displayed in log–log space. This curve fitting procedure has been described in detail recently by Schacher *et al.* (1981). The individual dV/dr values herein reported have all been calculated from the polynomial expressions appropriate to the specific measurement periods.

It has long been recognized that upon injection into the atmosphere a sea-salt droplet undergoes a rapid change in radius as it quickly attains the equilibrium size determined by its salt content and the ambient relative humidity (Keith and Arons 1954). To facilitate an intercomparison of the *Challenger* measurements taken under a range of relative humidities, and to make feasible the comparison of these JASIN aerosol data with earlier observations where sea-salt aerosols were often described in terms of dry radius or salt mass, every marine aerosol measurement presented in this paper has been adjusted in accord with the formula of Fitzgerald (1975) so that the reported radius and the associated volume fraction are those appropriate for a relative humidity of 80%.

The aerosol sampling aboard the *Hakuho Maru* was done with halide-ion-sensitive gelatin-coated film. In some instances the film was used in conjunction with a hand-operated jet impactor (Toba and Tanaka 1967; Chaen 1973) and in other instances a 3 to 5 mm wide ribbon of this film was mounted in a rod sampler (Chaen 1973; Toba and

Chaen 1973). After exposure to the marine atmosphere, and subsequent residence in a high humidity chamber, microphotographs of each such film were taken. The sizes of the silver chloride halos produced on the films where sea-salt droplets came to rest were measured on enlarged prints of these microphotographs, and the mass of sea-salt in each droplet was determined from the halo size using the calibration of Toba and Tanaka. Chaen indicates that a magnesium-oxide-coated ribbon was occasionally used in place of the gelatin-coated film in the rod sampler. Such oxide ribbons, after exposure, were placed under a vernier microscope and the dimensions of the craters produced by the sea-salt droplets were measured. From the known ratio of droplet diameter to pit diameter, 0·86, individual droplet sizes were determined. Aerosol samples were collected by these several means at a number of elevations aboard the *Hakuho Maru*, including 6 and 13 m above sea level.

Aerosol spectra from other sources which in this paper are compared with the characteristic spectra for various wind forces derived from the *Challenger* measurements are based upon data which were collected in a variety of ways.

Woodcock (1953) sampled marine aerosols by exposing glass slides (Woodcock and Gifford 1949) from aircraft. His measurements for all but the strongest wind category were carried out near cloud base in the vicinity of Hawaii. His force-12 data were collected in Florida during a tropical storm. The sample-bearing slides were returned to the laboratory and examined microscopically while held in an environment where the relative humidity was 90% to determine the dimensions of each sea-salt droplet. The individual salt masses were then computed using an isopiestic approach.

Metnieks (1958) made his aerosol measurements at an elevation of 1·5 m above a beach on the island of Inishmore in the mouth of Galway Bay, using a technique somewhat similar to that subsequently used by Chaen. The Inishmore sampling was done using a Casella® cascade impactor in association with gelatin-coated glass slides. Metnieks used silver nitrate to sensitize the gelatin while Chaen had used silver dichromate.

The GAMETAG experiment marine aerosol measurements reported by Patterson *et al.* (1980) were made with a P.M.S. aerosol spectrometer system, including both active scattering and forward scattering spectrometer probes, mounted in an Electra aircraft flown within the marine atmospheric boundary layer in remote areas of the Pacific Ocean where the relative humidity was observed to vary between 75 and 87%.

3. Observations of whitecaps and winds

In marked contrast to the variety characterizing the marine aerosol sampling procedures used in the various studies, the oblique photographic techniques employed aboard the *Hakuho Maru* (Toba and Chaen 1973) and the *Challenger* (Monahan *et al.* 1981) to record ocean whitecap cover, and the methods used to analyse the resulting colour transparencies, were quite similar. Whilst the number of photographs taken during each observation period and the orientation of the camera's field of view with respect to the wind varied between the two cruises, the individual whitecap cover values obtained on these cruises can with confidence be taken as directly comparable, since the ensemble of *Hakuho Maru* whitecap observations has been shown to be in "remarkable agreement" (Wu 1979b) with a large set of whitecap cover values (Monahan 1971) which had been obtained, as were the *Challenger* results, by following the measurement protocol set forth in Monahan (1969).

Wind speeds were measured at an elevation of 20 m aboard the *Hakuho Maru* (Toba and Chaen 1973) and at an elevation of 14 m aboard the *Challenger* and in both instances were extrapolated via neutral-stability logarithmic profile assumptions to obtain the equivalent winds at the standard elevation of 10 m.

The aerosol spectra reported by Woodcock (1953), Metnieks (1958) and Patterson *et al.* (1980) are each identified with an estimated Beaufort wind force. In the case of the GAMETAG experiment (Patterson *et al.*) the winds measured at aircraft height were used

in conjunction with profile assumptions to obtain estimates of the 11 m wind speed and these estimates were then converted to Beaufort forces. For the purposes of this paper all Beaufort wind force estimates have been converted to the corresponding wind speeds using a table of equivalents (Environment Canada 1975).

4. Variation of aerosol concentration with whitecap cover

The fraction of the marine air volume filled by aerosol droplets, as deduced from the measurements made at an elevation of 14 m aboard the *Challenger*, is positively correlated with concurrent ocean whitecap cover, even for the sub-micrometre radius droplets, as can be seen in Fig. 1(a). In this analysis the fractional whitecap cover associated with each aerosol measurement is derived from the analysis of a series of sea surface photographs taken during the relevant 3600 s aerosol sampling interval when such photographs were

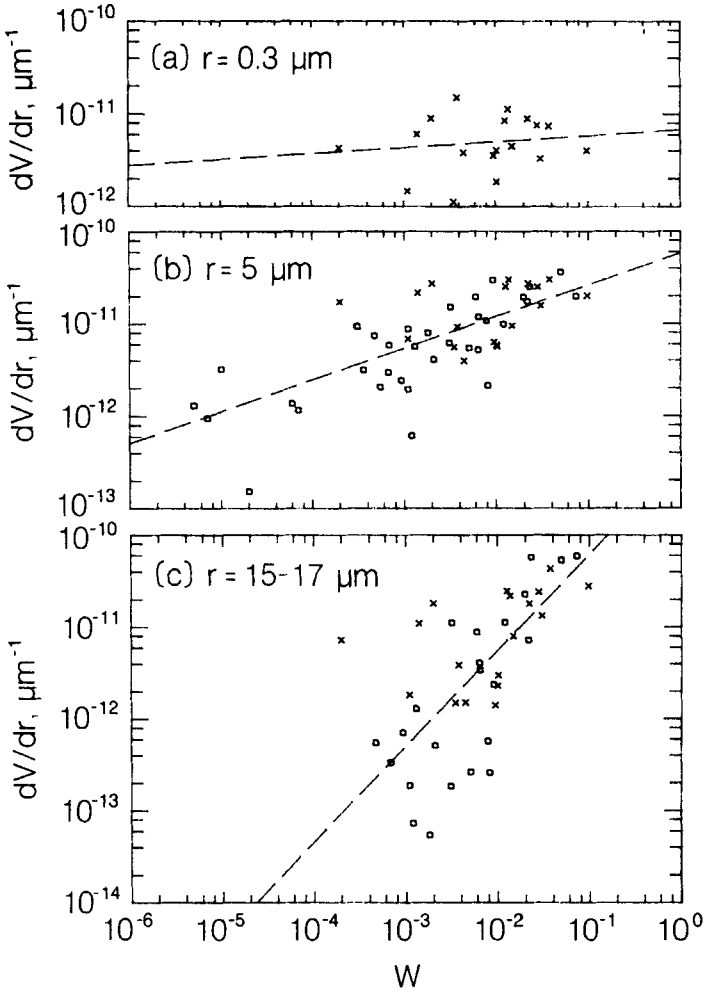

Figure 1. The fraction of the marine air volume filled by aerosol droplets, per unit increment droplet radius, *v.* ocean whitecap cover. Crosses: based on 14 m measurements aboard *Challenger*; open circles: from 6 m observations aboard *Hakuho Maru*; dashed lines: power-law descriptions obtained from applying robust bi-weight fitting to data in each of the three radii classes.

available, but in all instances the whitecap photographs were taken within two hours of the aerosol measurements with which they are identified. The power law

$$dV/dr = CW^{\gamma} \tag{1}$$

has been assumed to be a suitable description of the dependence of dV/dr, the fraction of the air occupied by droplets within a given radius interval, upon W, the whitecap cover and values of C and γ have been obtained by the application of two alternative statistical methods: the ordinary least squares (OLS) approach; and the technique of robust biweight fitting (RBF) described by Mosteller and Tukey (1977). Given that these procedures involve linear regression in log–log space, the data from any observation interval in which W, or dV/dr, was zero have of necessity been excluded. Noting the shortcomings of the OLS method when applied to data of this kind (Gaver 1979), the line drawn on Fig. 1(a) is that corresponding to the RBF fit, which represents a better description of the main body of the data (Monahan and O'Muircheartaigh 1980). The C and γ values obtained by the two methods are listed in Table 1, as is the standard deviation of γ, the slope.

TABLE 1. ALTERNATIVE $dV/dr(W)$ EXPRESSIONS

Droplet radius (μm)	log C		γ		
	OLS	RBF	OLS	RBF	σ_{γ}
0·3	−11·139	−11·167	0·086	0·065	0·071
5	−10·208	−10·234	0·361	0·343	0·084
15–17	−9·559	−9·164	0·860	1·043	0·156

A plot of dV/dr versus W, for 5 μm radius droplets, is presented in Fig. 1(b), where the data collected at 6 m aboard the *Hakuho Maru* are included along with the *Challenger* data. The synthesis of aerosol data from 6 m with that from 14 m is justified as only a very slight gradient in airborne sea-salt concentration exists in the intervening space (Blanchard and Woodcock 1980). The RBF fit represented by the line included on this figure, and the OLS and RBF entries for 5 μm in Table 1, were obtained by treating the two data sets as one extended set. On Fig. 1(c) are plotted dV/dr values for droplets of 15 μm radius based on the *Challenger* measurements, and for droplets of 17 μm radius derived from the *Hakuho Maru* observations. Given the uncertainties associated with the methods used to determine droplet size on the two cruises, and the large variability in the dV/dr values obtained for these large radii droplets due to the poor counting statistics, it is appropriate to treat these two droplet size categories as one. The RBF fit depicted on this figure, and the relevant entries in Table 1, are again based on the combined data set. The expected variability, or standard error, in the abscissa positions of the data points on the several panels of Fig. 1, i.e. in log W, is typically 0·22. This variability is due primarily to the fact that even in higher winds relatively few whitecaps contribute significantly to the whitecap cover determined from the typical aggregate of ten photographs. The expected variability in the ordinate positions of the data plotted on Fig. 1, i.e. in $\log(dV/dr)$, ranges from 0·1 for the 0·3 μm radius droplets (Fig. 1(a)) to 0·2 for the large (15–17 μm) droplets (Fig. 1(c)). In the case of the JASIN measurements, observational errors are due in large measure to ambiguities in the determination of droplet radii (Schacher *et al.* 1981), and, in the instance of the largest droplet category, to the few actual counts and the associated statistical shortcomings. It is apparent that the dependence of dV/dr upon whitecap cover increases with droplet radius.

Toba and Chaen (1973), in tabulating the results from the 1970 cruise of the *Hakuho Maru*, included a quantity henceforth referred to as N_{8+}, which is equivalent to the total number of aerosol particles per unit volume of air with radius, at 80% relative humidity, greater than 7·9 μm. The same quantity has been determined from the 1978 JASIN measurements, where the number of particles larger than 8 μm radius actually counted

during each 3600 s interval was employed, rather than the area under the polynomial curve derived in accord with the previously discussed smoothing procedure, in the calculation. This approach, which guaranteed that the JASIN N_{8+} values were independent of the spectrum of smaller particles, was a feasible one to adopt in this instance, where the particle counts, being summed over all particle radii categories above 8 μm, were typically larger than those measured in a single large radius category, and hence less subject to the large variations identified with small sample statistics. The variation of N_{8+} with whitecap cover, W, is portrayed in Fig. 2. A power law description was again assumed to be

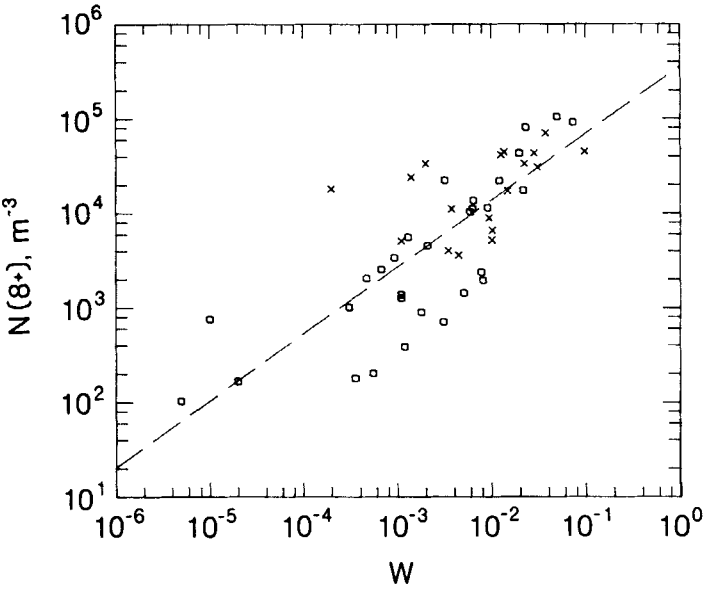

Figure 2. The number of aerosol particles per cubic metre of air with radii, at 80% relative humidity, greater than 7·9 μm, N_{8+}, *v.* ocean whitecap cover, W. Crosses: 14 m *Challenger* measurements; open circles: 6 m *Hakuho Maru* measurements; dashed line: power-law expression, $N_{8+} = 3{\cdot}59 \times 10^5 W^{0{\cdot}707}$, representing robust bi-weight fit to combined data set.

appropriate, and γ values of 0·664 and 0·707 were obtained by the respective application of the OLS and RBF procedures to the combined data set. As a consequence of the very rapid fall-off of the incremental number density, dN/dr, with increasing droplet radius, the whitecap dependence of N_{8+} can be expected to reflect closely the whitecap dependence of dN/dr, or dV/dr, evaluated for 8 μm droplets. In this regard it is to be noted that the RBF γ value for N_{8+}, 0·707, falls mid-way between the RBF γ value determined for dV/dr at 5 μm, 0·343, and at 15–17 μm, 1·043.

5. Wind speed dependence of whitecap cover and aerosol concentration

The dependence of ocean whitecap cover upon the 10 m wind speed has been considered at length in several recent publications, e.g. Wu (1979b) and Monahan and O'Muircheartaigh (1980). Using the preferred robust bi-weight fitting technique, assuming that the W dependence on wind speed, U, could be expressed in the form of another power law

$$W = \alpha U^{\lambda}, \tag{2}$$

TABLE 2. EXPRESSIONS FOR $W(U)$

Data set	Statistical method	log α	λ	Source
Hakuho Maru	exponent assumed	−5·810	3·75	Wu 1979b
Hakuho Maru	OLS	−5·255	3·3	Monahan and O'Muircheartaigh 1980
Hakuho Maru	RBF	−5·254	3·3	Monahan and O'Muircheartaigh 1980
Challenger	OLS	−5·246	3·27	Present study
Challenger	RBF	−5·265	3·31	Present study
Combined	OLS	−5·592	3·47	Present study
Combined	RBF	−5·347	3·31	Present study

Note: These α values are appropriate for use with Eq. (2) when U is expressed in $m\,s^{-1}$.

and treating the *Hakuho Maru* whitecap data of Toba and Chaen in the manner prescribed by Wu (1979b), Monahan and O'Muircheartaigh (1980) obtained a λ value of 3·3 (Table 2). Using the same statistical approach on the JASIN whitecap data resulted in a value of 3·31. This same value of 3·31 was also obtained when the RBF approach was applied to the combined *Challenger* and *Hakuho Maru* data sets while, contrary to the treatment of Wu (1979b), only those observations associated with null W values were omitted. While a detailed appreciation of the goodness-of-fit of the $W(U)$ expressions identified with various λ values is to be found in Monahan and O'Muircheartaigh, it can be stated here that a typical magnitude for the standard error associated with the λ values of Table 2 is 0·40. In Fig. 3 the whitecap cover determined for each observation interval aboard the *Hakuho Maru* and the *Challenger* is plotted against the simultaneous wind speed raised to the 3·3 power. The dashed line of slope unity in this figure corresponds to the bottom line of Table 2.

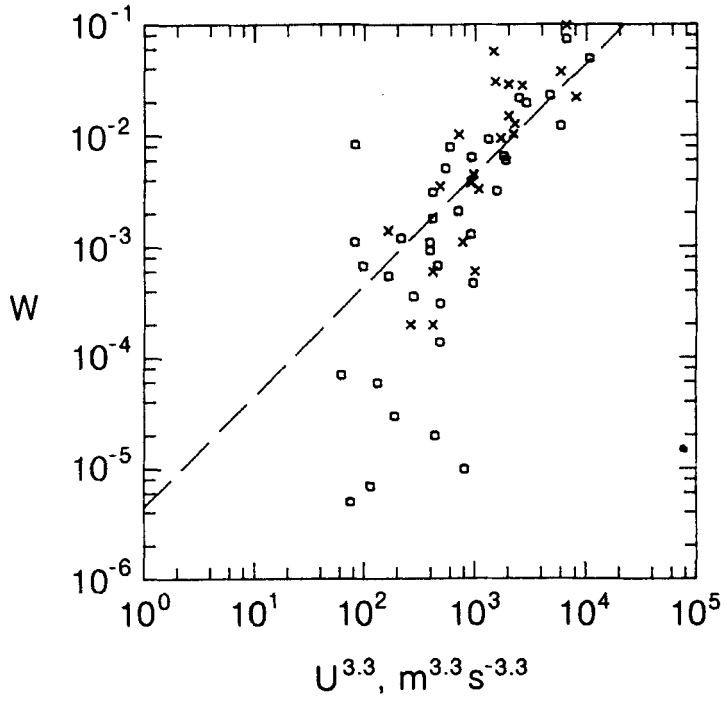

Figure 3. Ocean whitecap cover W *v.* 10 m wind speed, U, raised to the 3·3 power. Crosses: *Challenger*; open circles: *Hakuho Maru*; dashed line: power-law expression, $W = 4{\cdot}50 \times 10^{-6} U^{3{\cdot}31}$, based on the robust biweight fit to the composite data set.

The previously defined quantity N_{8+} can be taken as a measure of the concentration of the larger aerosol particles in the marine atmospheric boundary layer. If it is assumed that the dependence of N_{8+} on wind speed can be expressed as a power law similar to Eq. (2) then a λ value of 3·19 results from the OLS analysis of the composite *Hakuho Maru* and *Challenger* data set. A λ value of 3·23 is obtained by treating these same data using the RBF approach. In Fig. 4 the N_{8+} values are plotted against the pertinent wind speeds

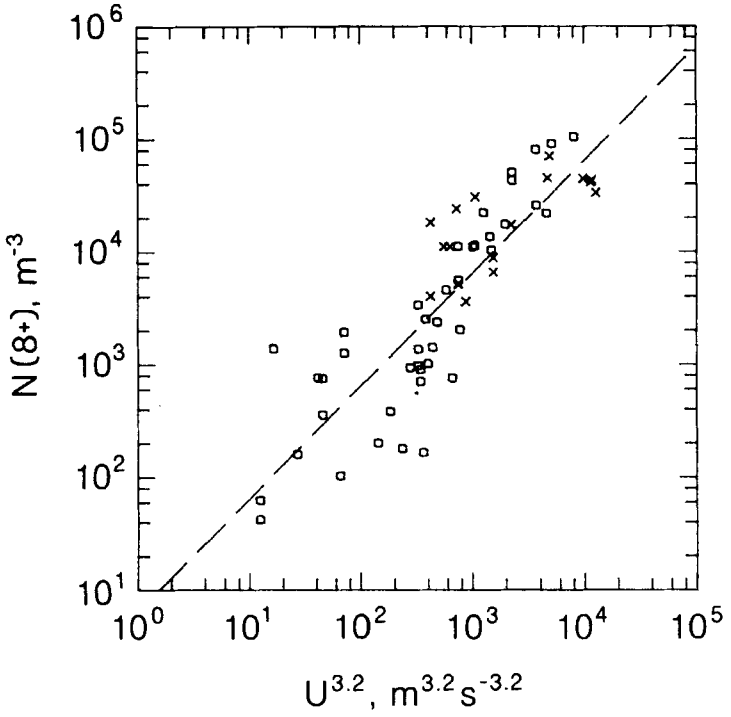

Figure 4. N_{8+}, the number of aerosol particles per cubic metre of air with radii, at 80% relative humidity, greater than 7·9 m, *v.* $U^{3\cdot2}$, the 10 m wind speed raised to the 3·2 power. Crosses: *Challenger*; open circles: *Hakuho Maru*; dashed line: robust bi-weight power-law expression, $N_{8+} = 6{\cdot}50\,U^{3\cdot23}$, for composite data set.

raised to the 3·2 power. The $N_{8+}(U)$ expression resulting from the RBF analysis of the combined data sets is represented in Fig. 4 by the dashed line of 45° slope.

The similar dependence upon wind speed reflected in the whitecap cover and N_{8+} values is quite striking, particularly when the RBF expressions are used in the comparison.

6. Variation of aerosol spectra with wind speed

Having in previous sections considered the variation with wind speed of the concentration of aerosol droplets of particular sizes, and of the total number of larger droplets, it is appropriate now to give explicit consideration to the change in the marine aerosol spectrum that results from a change in wind speed. In order to obtain such spectra from the JASIN measurements the mean 10 m wind speed for the 6 h period immediately preceding each 1200 s aerosol sampling interval was first determined. This wind-averaging period was selected as it has been found to be the one that gives the best correlation between marine atmospheric boundary layer visibility and wind speed (see Fairall *et al.*

(1983) for a discussion of aerosol equilibrium times). Then the actual aerosol counts in each size category obtained during all those sampling intervals associated with mean winds that fell within a particular $2\,m\,s^{-1}$ wide band of wind speeds were averaged to obtain a mean aerosol spectrum which could appropriately be identified with the mid-band wind speed. In this manner characteristic aerosol spectra for some nine wind speeds ($3\,m\,s^{-1}$, $5\,m\,s^{-1}$, $7\,m\,s^{-1}$, etc.) were constructed without resorting to the polynomial smoothing procedure used in defining the spectra from the measurements collected during individual sampling intervals. These spectra, expressed in terms of dV/dr *v.* r, and appropriate for a relative humidity of 80%, are contained in Fig. 5.

The aerosol spectra obtained by Woodcock (1953) from his near-cloud-base (600 to 800 m) measurements, and by Patterson *et al.* (1980) from other aircraft measurements also made well up in the marine atmospheric boundary layer, have been plotted in the same figure, having first been recast in terms of dV/dr *v.* r. The spectra derived from the shoreline measurements of Metnieks (1958), after suitable coordinate transformation, are

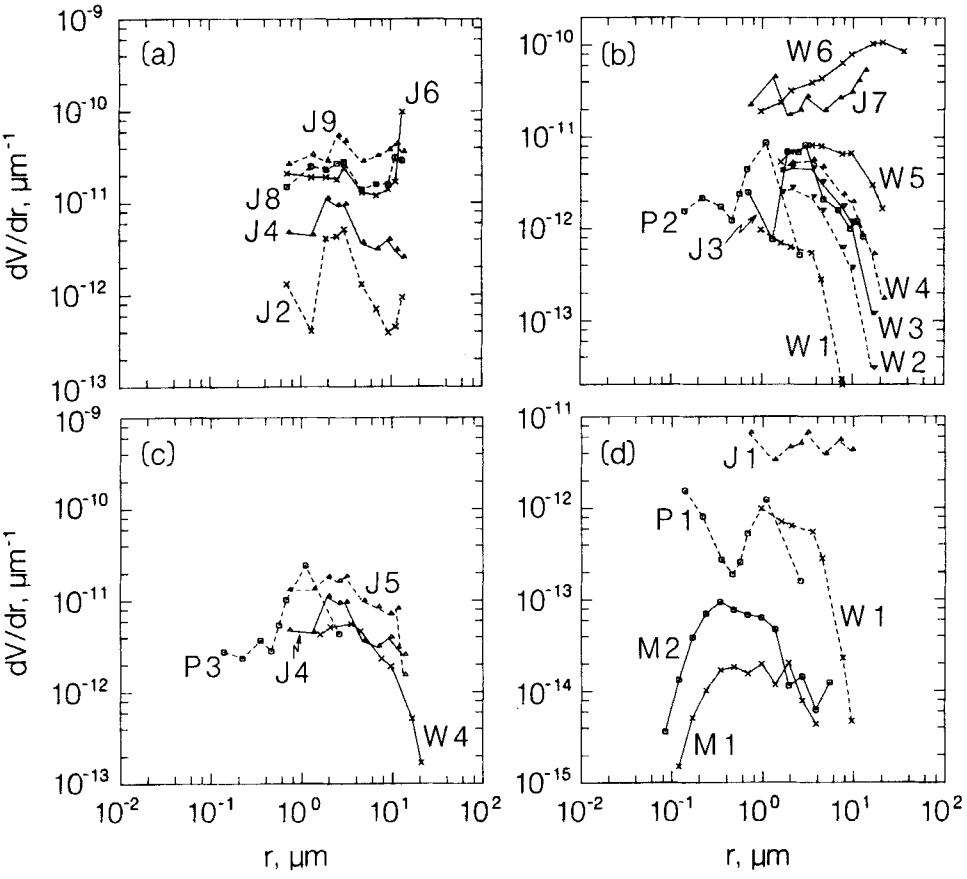

Figure 5. Marine aerosol spectra normalized to a relative humidity of 80%. On logarithmic axes the fraction of the marine air volume occupied by salt-water droplets which fall within a unit increment in radius has been plotted *v.* droplet radius. The J spectra, which are distributed among all four panels, were calculated from the JASIN measurements. J1: $3\,m\,s^{-1}$ winds; J2: $5\,m\,s^{-1}$; J3: $7\,m\,s^{-1}$; J4: $9\,m\,s^{-1}$; J5: $11\,m\,s^{-1}$; J6: $13\,m\,s^{-1}$; J7: $15\,m\,s^{-1}$; J8: $17\,m\,s^{-1}$; J9: $18\,m\,s^{-1}$ and higher. The W spectra (panels (b), (c) and (d)) were derived from Woodcock (1953). W1: $1{\cdot}0\,m\,s^{-1}$; W2: $4{\cdot}6\,m\,s^{-1}$; W3: $6{\cdot}7\,m\,s^{-1}$; W4: $9{\cdot}8\,m\,s^{-1}$; W5: $15{\cdot}4\,m\,s^{-1}$; W6: $35\,m\,s^{-1}$. The P spectra (panels (b), (c) and (d)) are based on the GAMETAG results (Patterson *et al.* 1980). P1: $2{\cdot}6\,m\,s^{-1}$; P2: $6{\cdot}7\,m\,s^{-1}$; P3: $9{\cdot}8\,m\,s^{-1}$. The M spectra (panel (d)) were determined from the Inishmore measurements (Metnieks 1958). M1 and M2: $2{\cdot}6\,m\,s^{-1}$ winds.

also included. All these published spectra have been adjusted to correspond to a relative humidity of 80%, except for the GAMETAG spectra for which corresponding humidity readings were not reported. Patterson *et al.* do state that the GAMETAG spectra are based on measurements collected when the humidity "ranged between 75 and 87%".

Each of the two consistent sets of aerosol spectra, the JASIN set and the set published by Woodcock, shows a general increase in amplitude with increasing wind speed. The near-sea-surface JASIN spectrum (Fig. 5(a)) seems to undergo a marked alteration in shape when the wind speed reaches $11\,m\,s^{-1}$. Above this speed the large droplet end seems to be more pronounced relative to the rest of the spectrum than at lower winds. In contrast to this, the near-cloud-base spectrum of Woodcock (Fig. 5(b)) shows a continuous modification of shape, with the large droplet end becoming progressively more pronounced as the wind speed increases to hurricane strength. The ratio of 14 m values to cloud base values of dV/dr for 11 μm radius droplets is seen to increase from 2·0 at a wind speed of $7\,m\,s^{-1}$ to 4·3 at $11\,m\,s^{-1}$, and to increase further to 8·2 at $15\,m\,s^{-1}$, in accord with the foregoing observations. While the spectra obtained near the sea surface and near cloud base are quite similar at moderate wind speeds such as $6{\cdot}7\,m\,s^{-1}$ (spectra J3 and W3 in Fig. 5(b)) and perhaps even at $10\,m\,s^{-1}$ (J4 or J5 and W4 in Fig. 5(c)), when the winds reach $15\,m\,s^{-1}$ the near-sea-surface spectrum has a much greater amplitude across the spectrum than does the near-cloud-base one (J7 and W5 in Fig. 5(b)).

As was noted by Patterson *et al.* (1980), the GAMETAG aerosol spectra appear to be shifted toward smaller drop size relative to the Woodcock spectra. This is manifest from a comparison of spectra P2 and W3 in Fig. 5(b), or of P3 and W4 in Fig. 5(c). This same apparent offset is discerned when the GAMETAG spectra are compared with the pertinent JASIN ones, e.g. P2 *v.* J3 in Fig. 5(b) or P3 *v.* J4 in Fig. 5(c).

When the various aerosol spectra associated with wind speeds less than about $4\,m\,s^{-1}$, the speed identified with the onset of whitecapping (Monahan 1971), are compared (Fig. 5(d)) the great diversity among these low wind speed spectra is striking.

7. Conclusions

The increase with increasing droplet radius of the dependence of dV/dr on whitecap cover illustrated in Fig. 1 and Table 1 is consonant with two physical considerations. During the high-wind large-whitecap-cover intervals of pronounced aerosol generation relatively more small droplets than large droplets are injected into the atmosphere (Monahan *et al.* 1982). In addition, the gravitational-settling and turbulent-deposition velocities for small droplets are less than for large droplets. These two considerations lead to a large atmospheric reservoir of small droplets, which is depleted but slowly during the lull periods subsequent to major generation episodes, and as a consequence is only modestly correlated with the immediate aerosol generation rate, i.e. with the instantaneous ocean whitecap cover. Conversely, the atmospheric reservoir of large droplets is never great, and after periods of high production the concentration of these droplets falls off quickly, resulting in the high correlation found between simultaneous measurements of large particle concentration and whitecap cover.

The gravitational-settling velocities (V_g) of the droplets whose whitecap dependence is illustrated in Fig. 1, and the turbulent-deposition velocities (V_t) for these droplets when the wind speed is $6\,m\,s^{-1}$, are listed in Table 3. The disparity of droplet residence times is apparent from a consideration of the times listed in this table for gravitational fall-out (T_g) and for turbulent deposition (T_t) from the several measurement elevations, i.e. 14 m for the JASIN experiment and 600 m for the earlier observations of Woodcock (1953). The 0·3 μm radius droplets will take from several days to several months to fall from the heights considered, whilst the 15 μm radius droplets will fall from these heights to the sea surface in a matter of from six minutes to five hours.

TABLE 3. DROPLET DEPOSITION RATES

Radius (μm)	0·3	5	15
V_g (m s^{-1})	$1{\cdot}38 \times 10^{-5}$	$3{\cdot}00 \times 10^{-3}$	$2{\cdot}71 \times 10^{-2}$
V_t (m s^{-1})	$7{\cdot}85 \times 10^{-5}$	$7{\cdot}64 \times 10^{-3}$	$3{\cdot}55 \times 10^{-2}$
T_g (14 m) (s)	$1{\cdot}01 \times 10^{6}$	$4{\cdot}67 \times 10^{3}$	$5{\cdot}17 \times 10^{2}$
T_t (14 m) (s)	$1{\cdot}78 \times 10^{5}$	$1{\cdot}83 \times 10^{3}$	$3{\cdot}94 \times 10^{2}$
T_g (600 m) (s)	$4{\cdot}34 \times 10^{7}$	$2{\cdot}00 \times 10^{5}$	$2{\cdot}21 \times 10^{4}$
T_t (600 m) (s)	$7{\cdot}64 \times 10^{6}$	$7{\cdot}85 \times 10^{4}$	$1{\cdot}69 \times 10^{4}$

For those droplet categories (Figs. 1(b, c), 2) for which there are East China Sea measurements to compare with the observations taken in the NE Atlantic Ocean near Rockall, a significantly stronger whitecap dependence is exhibited in each instance by the East China Sea data. This becomes apparent when, for example, the γ value (Eq. 1) obtained for 5 μm radius droplets by application of the RBF method to the NE Atlantic data alone, 0·113, is compared with the γ value for the same droplet category obtained by the identical method from the East China Sea observations, 0·362. This is a reflection of the fact that during the East China Sea cruise of the *Hakuho Maru* all the high-wind and large-whitecap-cover observations were associated with one coherent storm, Typhoon *Oruga*, whilst during the JASIN cruise of the *Challenger* the NE Atlantic Ocean was subjected to the passage of a number of fronts and small storms. Thus the wind speed and whitecap cover experienced during the *Hakuho Maru* cruise varied more slowly than did the same quantities during the JASIN experiment, and as a result the aerosol reservoir of the marine atmospheric boundary layer was better able to adjust with the slow changes of whitecap cover and wind speed associated with the East China Sea observations.

Whilst the dependence of low elevation large droplet concentration, N_{8+}, on whitecap cover would appear, from the RBF line of slope 0·707 reproduced in Fig. 2, to be less than linear, the markedly similar wind dependence demonstrated by the combined whitecap cover data set (RBF λ of 3·31, Fig. 3) and by the composite N_{8+} values (RBF λ of 3·23, Fig. 4) does suggest that the concentration in the marine atmospheric boundary layer of large aerosol droplets is essentially proportional to the instantaneous whitecap cover of the underlying ocean. The same conclusion was reached by Toba and Chaen (1973), based on their observation that the whitecap cover, W, and large aerosol concentration, N_{8+}, measured during the *Hakuho Maru* cruise could both be described by

$$X = \beta(u_* L/\nu)^{3/2} = \beta(UL/\nu)^{3/2} C_D^{3/4} \tag{3}$$

with $X = N_{8+}$, $\beta = B_1$ or $X = W$, $\beta = B_2$; u_* being the friction velocity, L the significant wavelength, ν the kinematic viscosity of air, and C_D the 10 m drag coefficient.

That the results obtained by directly comparing N_{8+} with W (Fig. 2), and by inferring indirectly their inter-relationship from the similar dependencies on U (Figs. 3 and 4), or on $u_* L/\nu$, are not entirely consistent reflects in part the 'noisy' nature of these data. It is clear that neither W, nor N_{8+}, can be fully described in terms of U, or, alternatively, $u_* L/\nu$. Instantaneous whitecap cover is not only a function of wind speed, but also of wind duration and fetch, the gravitational stability of the lower atmosphere (Monahan 1969) and, in shallow regions, the bathymetry of the sea bed. The temperature of the surface sea-water affects the rise time of whitecap bubbles and hence the effective lifetime of individual whitecaps (Monahan and O'Muircheartaigh 1980). Thus in colder, more viscous, waters the instantaneous whitecap cover will be greater than in warmer seas under the same meteorological conditions, i.e. when the same number of waves are breaking per unit time per unit area. The presence and extent of organic material on the sea surface will affect bubble stability and hence whitecap lifetimes (Abe *et al.* 1963) and also will alter the efficiency with which bubbles when they eventually burst produce droplets. Preliminary results (Monahan 1979) suggest that an organic film can decrease the aerosol production efficiency of a bursting bubble by a factor of two or more. Likewise, the humidity-adjusted low elevation concentration of large aerosol droplets, N_{8+},

depends not only on instantaneous wind speed and the wind history, but also on the gravitational stability of the lower atmosphere (Goroch *et al.* 1979), the presence and strength of the inversion capping the marine atmospheric boundary layer (Fairall *et al.* 1982) and such mesoscale meteorological considerations as advection, subsidence and washout via rain.

The rapid increase in the concentration of large aerosol droplets, N_{8+}, with increasing wind speed depicted in Fig. 4 exceeds the increase in aerosol concentration with increasing wind speed predicted by the semi-empirical model of Wells *et al.* (1977), which contains several wind-dependent coefficients and exponents. This is apparent when the wind dependence of the aerosol optical extinction coefficient obtained from the JASIN aerosol measurements is compared with the wind dependence of the extinction coefficient derived from the model of Wells *et al.*, as has recently been done by Fairall *et al.* (1982).

Lovett (1978), analysing measurements of airborne sea-salt taken in the NE Atlantic Ocean aboard weather ships, concluded that the mass concentration of airborne salt, m, varied with wind speed as shown in Eq. (4)

$$m = \delta e^{0.16U}, \tag{4}$$

where U is the wind speed in $m\,s^{-1}$. This formula implies that as the wind speed increases from 5 to 15 $m\,s^{-1}$, the concentration of airborne salt increases by a factor of 4·95. This is somewhat greater than the increase by a factor of 3·48 in the concentration of droplets of 5 μm radius which can be inferred for the same shift in wind speeds from the results presented in Figs. 1(b) and 3, but markedly less than the increase in concentration which the results of the present study suggest would occur in the concentration of larger droplets (8 or 15 μm radius) if the wind speed underwent the same alteration.

The relative similarity in the shape of the near-sea-surface JASIN aerosol spectra associated with wind speeds up to 9 $m\,s^{-1}$ (Figs. 5(a, b, c)), and the near proportionality manifest between large droplet concentration, N_{8+}, and whitecap cover, W, are consistent with the model for sea surface aerosol generation described by (Monahan *et al.* 1982)

$$dF_0/dr = (dE/dr)\tau^{-1} W(U), \tag{5}$$

where dF_0/dr represents the aerosol production per increment droplet radius per unit time per unit area of the ocean, dE/dr is the number of aerosol droplets per radius increment produced during the decay of a unit area of whitecap, τ the characteristic decay time for an individual whitecap and $W(U)$ the oceanic whitecap cover at wind speed U. In this model dE/dr is assumed not to be a function of wind speed.

The pronounced enhancement of the large droplet end of the low elevation aerosol spectra identified with wind speeds of 11 $m\,s^{-1}$ and greater reflects the introduction of a supplementary droplet production mechanism when the winds reach the 9 to 11 $m\,s^{-1}$ range, a process associated with the presence at high wind speeds of streaks (Ross and Cardone 1974) or spume lines. This additional droplet production mechanism is the mechanical tearing away of wave crests (Monahan and Muircheartaigh 1980). Such mechanical disruption of bulk water favours, from energetic considerations, the formation of quite large droplets (Tonkonogov *et al.* 1976). These findings suggest that an additional term needs to be added to the sea surface aerosol source function (Eq. (5)) to broaden its applicability to embrace the high wind speed, spume production, situations.

The increased disparity with increasing wind speed between the amplitudes of the near-sea-surface and near-cloud-base aerosol spectra already remarked upon is a consequence of the fact that at the higher speeds more large droplets, which fall out before they can be mixed effectively throughout the marine atmospheric boundary layer, are produced. It also reflects the observation that as the wind freshens the turbulent mixing, which tends to distribute aerosol droplets evenly throughout the boundary layer, increases, but not as rapidly as the sea surface aerosol generation increases with wind speed. Thus at higher wind speeds the wind must blow longer than at lower wind speeds before an equilibrium vertical distribution of aerosols is reached. Such sustained periods of high

winds are not always encountered. The present observations are in accord with the positive wind dependence of the vertical gradient of atmospheric salt concentration described by Blanchard and Woodcock (1980).

The great variation noted amongst the aerosol spectra associated with wind speeds less than those required to produce whitecapping (Fig. 5(d)) is a consequence of the fact that these spectra are reflections of earlier winds elsewhere, not of the immediate local wind.

Acknowledgments

The investigation of whitecap–aerosol inter-relationships at the Naval Postgraduate School and at University College, Galway, is supported by the Office of Naval Research via work request N00014-81-WR-10135 and grant N00014-78-G-0052 respectively. This paper was begun while the first author (E.C.M.) occupied the G. J. Haltiner Research Chair in Meteorology at NPS, which is supported by the Naval Air Systems Command (AIR 370). The contributions of G. E. Schacher to all phases of JASIN aerosol study are acknowledged with gratitude. The authors also gratefully acknowledge the assistance provided during this study by E. Murphy, J. Boyle, E. Dockery, V. Lopez and M. McDermet.

References

Abe, T., Ono, T. and Kishino — 1963 — A fundamental study on the prevention of the salty damages due to the foaming of sea water (preliminary report), *J. of the Ocean. Soc. of Japan*, **18**, 185–192.

Blanchard, D. C. — 1963 — The electrification of the atmosphere by particles from bubbles in the sea, *Progress in Oceanography*, **1**, 71–202.

Blanchard, D. C. and Woodcock, A. H. — 1957 — Bubble formation and modification in the sea and its meteorological significance, *Tellus*, **9**, 145–158.

1980 — The production, concentration, and vertical distribution of the sea-salt aerosol, *Annals of the New York Academy of Sciences*, **338**, 330–347.

Chaen, M. — 1973 — Studies on the production of sea-salt particles on the sea surface, *Memoirs of the Faculty of Fisheries, Kagoshima University*, **22**, 49–107.

Cipriano, R. J. and Blanchard, D. C. — 1981 — Bubble and aerosol spectra produced by a laboratory 'breaking wave', *J. of Geo. Res.*, **86**, 8085–8092.

Coantic, M. — 1980 — Mass transfer across the ocean-air interface: small scale hydrodynamic and aerodynamic mechanisms, *PCH Physico-Chemical Hydrodynamics*, **1**, 249–276.

Environment Canada — 1975 — *State of sea photographs for the Beaufort wind scale*, Atmospheric Environment Service, Information Canada, Ottawa.

Fairall, C. W., Davidson, K. L. and Schacher, G. E. — 1982 — Meteorological models for optical properties in the marine atmospheric boundary layer, *Opt. Eng.* (in press).

1983 — An analysis of the surface production of sea-salt aerosols, *Tellus* (in press).

Fitzgerald, J. W. — 1975 — Approximation formulas for the equilibrium size of an aerosol particle as a function of its dry size and composition and the ambient relative humidity, *J. of Applied Met.*, **14**, 1044–1049.

Gaver, D. P. — 1979 — *Statistical methods of probable use for understanding remote sensing data, Tech Rept. NPS-79-020*, Naval Postgraduate School, Monterey

Goroch, A., Burk, S. and Davidson, K. L. — 1979 — Stability effects on aerosol size and height distributions, *Tellus*, **31**, 1–6.

Hayami, S. and Toba, Y. — 1958 — Drop production by bursting of air bubbles on the sea surface: (1) experiments at still water surface, *J. of the Ocean. Soc. of Japan*, **14**, 145–150.

Keith, C. H. and Arons, A. B. — 1954 — The growth of sea-salt particles by condensation of atmospheric water vapor, *J. of Met.*, **11**, 173–184.

Kientzler, C. F., Arons, A. B., Blanchard, D. C. and Woodcock, A. H.	1954	Photographic investigation of the projection of droplets by bubbles bursting at a water surface, *Tellus*, **6**, 1–7.
Lovett, R. F.	1978	Quantitative measurement of airborne sea-salt in the North Atlantic, *Tellus*, **30**, 358–364.
Metnieks, A. L.	1958	The size spectrum of large and giant sea-salt nuclei under maritime conditions, *Geophys. Bulletin 15*, Dublin Institute for Advanced Studies.
Monahan, E. C.	1969	Fresh water whitecaps, *J. of the Atmos. Sciences*, **26**, 1026–1029.
	1971	Oceanic whitecaps, *J. of Phys. Ocean.*, **1**, 139–144.
	1979	*The influence of whitecaps on the marine atmosphere, Tech. Rept. 1 to O.N.R.*, University College, Galway.
Monahan, E. C., Davidson, K. L. and Spiel, D. E.	1982	Whitecap aerosol productivity deduced from simulation tank measurements, *J. of Geophys. Res.* **87**, 8898–8904.
Monahan, E. C. and O'Muircheartaigh, I.	1980	Optimal power-law description of oceanic whitecap coverage dependence on wind speed, *J. of Phys. Ocean.*, **10**, 2094–2099.
Monahan, E. C., O'Muircheartaigh, I. G. and FitzGerald, M. P.	1981	Determination of surface wind speed from remotely measured whitecap coverage, a feasibility assessment, *Proceedings of an EARSeL-ESA Symposium, Voss, Norway, 19–20 May 1981*, European Space Agency Special Pub. 167, 103–109.
Moore, D. J. and Mason, B. J.	1954	The concentration, size distribution, and production rate of large salt nuclei over the oceans, *Quart. J. R. Met. Soc.*, **80**, 583–590.
Mosteller, F. and Tukey, J. W.	1977	*Data Analysis and Regression: a Second Course in Statistics*, Addison-Wesley, Reading.
Patterson, E. M., Kiang, C. S., Delany, A. C., Wartburg, A. F., Leslie, A. C. D. and Huebert, B. J.	1980	Global measurements of aerosols in remote continental and marine regions: concentrations, size distributions and optical properties, *Journal of Geophysical Research*, **85**, 7361–7376.
Pinnick, R. G. and Auvermann, J. J.	1979	Response characteristics of Knollenberg light-scattering aerosol counters, *J. of Aerosol Science*, **10**, 55–74.
Ross, D. B. and Cardone, V.	1974	Observations of oceanic whitecaps and their relation to remote measurements of surface wind speed, *J. of Geophys. Res.*, **79**, 444–452.
Schacher, G. E., Davidson, K. L., Fairall, C. W. and Spiel, D. E.	1981	Calculation of optical extinction from aerosol spectral data, *Applied Optics*, **20**, 3951–3957.
Sigerson, G.	1870	Micro-atmospheric researches, *Proceedings of the Royal Irish Academy, Series 2, 1-Science*, 13–30.
Toba, Y. and Chaen, M.	1973	Quantitative expression of the breaking of wind waves on the sea surface, *Records of Oceanographic Works in Japan*, **12**, 1–11.
Toba, Y. and Tanaka, M.	1967	Simple technique for the measurement of giant sea-salt particles by use of a hand-operated impactor and chloride reagent film, *Special Contributions, Geophysical Institute, Kyoto University*, **7**, 111–118.
Tonkonogov, M. P., Kim, S. V., Klimchuk, A. Ye. and Lekht, Yu. I.	1976	Effect of concentration of the dispersed liquid on the particle-size distribution in aerosol flows, *Fluid Mechanics-Soviet Research*, **5**, 157–161. (Orig. pub. in *Izvestiya Vuzov-Energetika*, **3**, 141–144, 1976.)
Wells, W. C., Gal, G. and Munn, M. W.	1977	Aerosol distributions in maritime air and predicted scattering coefficients in the infrared, *J. of App. Opticals*, **16**, 654–659.
Woodcock, A. H.	1953	Salt nuclei in marine air as a function of altitude and wind force, *J. of Met.*, **10**, 362–371.
Woodcock, A. H. and Gifford, M. M.	1949	Sampling atmospheric sea salt, *J. of Marine Res.*, **8**, 177–197.
Wu, J.	1979a	Spray in the atmospheric surface layer: review and analysis of laboratory and oceanic results, *J. of Geophys. Res.*, **84**, 1693–1704.
	1979b	Oceanic whitecaps and sea state, *J. of Phys. Ocean.*, **9**, 1064–1068.